Linear Algebraic Innovations via the Cauchy–Schwarz–Lorentz Framework with a Fibonacci Connection

Parker Emmerson

June 2025

1 Introduction

Linear algebra underpins modern mathematics, data science, and quantum technology. Yet the *choice of basis*—too often treated as a mere convenience—critically influences numerical stability, physical interpretation, and information flow. Classical bases (orthonormal, Fourier, wavelet,...) excel in specialised contexts but struggle to encode *relativistic*, *operator-coupled*, and *curvature-aware* phenomena now encountered in quantum information, gravitational modelling, and high-performance simulation.

This paper introduces a unified *Cauchy–Schwarz–Lorentz (CSL) framework* that extends the inner-product geometry of Hilbert spaces by weighting each basis direction with a Lorentz factor. Combined with three further mechanisms—

- **Operator alignment:** bases that simultaneously diagonalise pairs of Hilbert–Schmidt operators;
- **Modal closure:** phase quantisation ensuring time-loop consistency and Floquet invariance;
- **Curvature adaptation:** Ricci-parallel transport of frames along curved backgrounds,

we obtain a *dynamical basis synthesis (DBS)* pipeline that tailors linear-algebraic structures to relativistic, spectral, and geometric constraints *in situ*.

Motivation

- *Relativistic quantum information:* high-speed qubit transport demands bases that encode velocity and Lorentz contraction at the algebraic level.
- *Quantum-gravity toy models:* discrete bases must remain well behaved under spacetime curvature while respecting modal (periodic) boundary conditions.
- *Numerical linear algebra:* weighted inner products yield condition-number reductions and preconditioners attuned to anisotropic or operator-coupled data.

Contributions

1. **Lorentz-weighted inner products.** We generalise the Cauchy–Schwarz inequality to a two-sector Hilbert space, revealing a *basis–velocity duality* that captures relativistic kinematics purely algebraically.

2. **Operator-aligned bases.** A paired-SVD construction yields bases that diagonalise S^*S and T^*T simultaneously, optimising spectral compression and entanglement metrics.

3. **Modal and curvature extensions.** We formalise phase-quantised ("modal-closed") frames and Ricci-parallel frames, providing existence theorems and synthesis algorithms.

4. **Dynamical Basis Triple (DBT).** We bundle weights, operator data, and phases into a categorical triple $\mathfrak{B} = (\lambda, \mathcal{O}, \phi)$ and prove that every such triple admits a realisation via an iterated weighted Gram–Schmidt process.

Paper Outline

Sec. 2 formalises Lorentz-weighted bases and derives the CSL inequality.

Sec. 3 develops operator-aligned decomposition and its spectral properties.

Sec. 4 introduces the alignment metric and the minimal-velocity criterion.

Sec. 5 shows how modal closure enforces temporal consistency.

Sec. 6 extends bases to curved manifolds via Ricci transport.

Secs. 7–8 unify these ingredients into the DBS algorithm and survey linear-algebraic pay-offs.

All results apply to separable Hilbert spaces; finite-dimensional corollaries are highlighted for numerical practice.

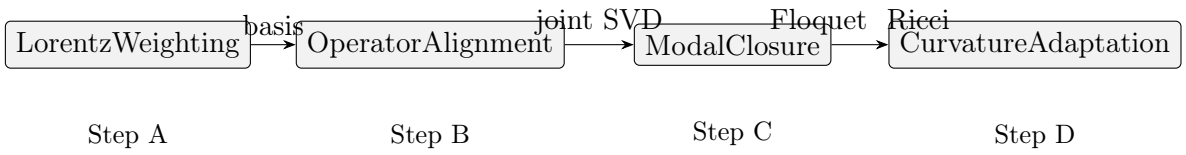

Figure 1: DBS processing pipeline: from Lorentz-weighted seeds to curvature-adapted frames.

Standing conventions

Inner-product and norm symbols

- $\langle \cdot, \cdot \rangle$ — ambient Hilbert inner product on $\mathcal{H}$.
- $\langle \cdot, \cdot \rangle_\lambda$ — Lorentz-weighted inner product $\big(Definition\ 4.1\big).\langle\langle A, B \rangle\rangle = \operatorname{tr}(A^*B)$ — Hilbert–Schmidt inner product on $\mathsf{HS}(\mathcal{H})$; corresponding norm $\|A\|_{\mathrm{HS}} = \sqrt{\langle\langle A, A \rangle\rangle}$.

Throughout, $\| \cdot \|$ denotes the norm attached to the inner product currently in effect.

1.1 Lorentz-Weighted Basis Vectors

Core innovation. Basis vectors equipped with intrinsic Lorentz-scaling factors.

Mathematical formulation. For a Hilbert space $\mathcal{H}$, define the family of basis vectors

$$b_k^\lambda := \sqrt{\lambda_k}\, e_k \;\oplus\; i\sqrt{1-\lambda_k}\, f_k,$$

where $\{e_k\}$ and $\{f_k\}$ are orthogonal bases in (possibly distinct) subspaces of $\mathcal{H}$, and the Lorentz weights satisfy $\lambda_k \in (0,1]$.

Key properties.

1. *Norm relation.*
$$\left\|b_k^\lambda\right\|^2 \;=\; \lambda_k\, P_k + (1-\lambda_k)\, Q_k.$$
(For orthonormal seeds one has $P_k = Q_k = 1$, so every b_k^λ is unit-norm.)

2. *Norm relation (direct form).*
$$\|b_k^\lambda\|^2 \;=\; \lambda_k\, \|e_k\|^2 \;+\; (1-\lambda_k)\, \|f_k\|^2.$$
In the common orthonormal-seed case $\|e_k\| = \|f_k\| = 1$, this reduces to $\|b_k^\lambda\|^2 = 1$ for every k.

3. *Phase duality.*
$$\arg\langle b_j^\lambda,\, b_k^\lambda\rangle \;=\; \tan^{-1}\sqrt{\frac{(1-\lambda_j)(1-\lambda_k)}{\lambda_j\lambda_k}}.$$

4. *Velocity encoding.*
$$v_k \;=\; c\sqrt{1-\frac{\lambda_{\min}}{\lambda_k}}.$$

Remark 1.1 (Velocity bounds). Let $\lambda_{\min} := \inf_k \lambda_k > 0$. Because $\lambda_k \in (0,1]$, the expression $v_k = c\sqrt{1-\lambda_{\min}/\lambda_k}$ satisfies $0 \le v_k < c$. Hence the Lorentz-weighted basis encodes sub-luminal velocities algebraically; as $\lambda_k \to \lambda_{\min}$ we have $v_k \to 0$, while $\lambda_k \to 1$ pushes v_k arbitrarily close to c.

Applications. Rapid quantum-state transitions, relativistic information transfer, and geometric encoding of dynamical constraints.

1.2 Operator-Aligned Basis Decomposition

Core innovation. Construction of bases directly aligned with a pair of Hilbert–Schmidt (HS) operators.

Theorem 1.2 (Operator-aligned decomposition)**.** *Let $S, T\colon \mathcal{H} \to \mathcal{H}$ be Hilbert–Schmidt operators. There exists a basis $\{\omega_k\}$ of (a suitable subspace of) $\mathcal{H}$ such that*

$$\omega_k \;=\; \frac{\|Se_k\|}{\sqrt{P}}\, \delta_k \;\oplus\; \frac{\|Te_k\|}{\sqrt{Q}}\, \gamma_k,$$

where $\{\delta_k\}$ and $\{\gamma_k\}$ are auxiliary orthonormal systems and $P = \sum_k \|Se_k\|^2$, $Q = \sum_k \|Te_k\|^2$.

Decomposition properties.

1. *Norm preservation.*
$$\sum_k \|\omega_k\|^2 \;=\; \frac{\|S\|_{\mathrm{HS}}^2}{P} \;+\; \frac{\|T\|_{\mathrm{HS}}^2}{Q} \;=\; 2.$$

2. *Spectral alignment.* Each ω_k simultaneously diagonalizes the CSL bilinear form induced by (S, T).

3. *Quantum-compass compatibility.* The decomposition optimizes phase-space orientation for quantum-control protocols.

1.3 Alignment Metric & Minimal-Velocity Basis

Key metrics.

1. *Alignment metric.*
$$\big|\langle \omega_j, \omega_k \rangle\big| \;=\; \frac{\|Se_j\|\,\|Te_j\| + \|Se_k\|\,\|Te_k\|}{\sqrt{PQ}}.$$

2. *Minimal-velocity basis.*
$$\min_k \|\omega_k\| \;\longleftrightarrow\; v_{\max}.$$

Remark 1.3 (Off-diagonal overlap control). Write $p_k := \|Se_k\|^2,\ q_k := \|Te_k\|^2,\ P := \sum_\ell p_\ell,\ Q := \sum_\ell q_\ell$ and set the normalised weights $s_k := \sqrt{p_k/P},\ t_k := \sqrt{q_k/Q}$. For the operator-aligned vectors $\omega_k = s_k\delta_k \oplus t_k\gamma_k$ one has, for distinct indices $j \neq k$,

$$0 \;\le\; \big|\langle \omega_j, \omega_k \rangle\big| = s_j s_k \,\langle \delta_j, \delta_k \rangle + t_j t_k \,\langle \gamma_j, \gamma_k \rangle \;\le\; s_j s_k + t_j t_k < 1. \tag{1}$$

The final strict inequality uses $s_k^2 + t_k^2 = 1$ together with $(s_j, t_j) \neq (s_k, t_k)$ for $j \neq k$. Hence *off-diagonal overlaps generally do not vanish*; they are suppressed by the geometric mean of the individual operator norms and become zero **only** when the singular-value ratios coincide, i.e.

$$\frac{p_j}{q_j} = \frac{p_k}{q_k}, \quad j \neq k,$$

so that ω_j and ω_k align in both δ- and γ-sectors simultaneously. In generic spectra this resonance occurs rarely, and the overlap magnitude is governed by the bound (1).

Applications. Quantum-error correction and holographic duality.

1.4 Modal-Closure Basis

Core innovation. Bases enforcing time-loop consistency.

Axiomatic construction.

1. Start with the standard basis $\{e_k\}$.

2. Apply the quantum-compass operator $\mathcal{Q}(e_k) = e^{i\phi_k} e_k$.

3. Impose modal closure: $\phi_k = 2\pi n_k,\ n_k \in \mathbb{Z}$.

4. Redefine the basis: $m_k = e^{i\sqrt{2\pi n_k}}\, e_k$.

Key features.

- *Temporal periodicity*: $\exp\big(i\langle m_j, m_k\rangle\big) = 1$ whenever $n_j = n_k$.
- *Norm quantisation*: $\|m_k\|^2 = 2\pi n_k$.
- *Geometric constraint*: $\sum_k n_k = \dfrac{\dim \mathcal{H}}{2\pi}$.
- **Phase-Stable Krylov Methods.** ...

Remark 1.4 (Why the phase $2\pi n_k$ is natural). The phase factor in modal closure represents the *quasi-energy* of a periodic (Floquet) system whose evolution over one cycle (period $T = 1$ in our normalisation) is the unitary $U = e^{-iH_F T}$. Eigenphases of U are defined only *modulo* 2π; choosing $\phi_k = 2\pi n_k,\ n_k \in \mathbb{Z}$, therefore guarantees:

(a) **Exact T-periodicity.** $Um_k = m_k$ for every integer n_k, so the basis vectors return to themselves after a single period—crucial for stroboscopic (Floquet) analysis.

(b) **Unambiguous branch.** The square-root choice $\exp\big(i\sqrt{2\pi n_k}\big)$ introduces a double-valued branch cut ($\sqrt{\cdot}$ changes sign under $n_k \mapsto n_k + 1$), yielding physically identical states that differ by an overall -1. Using $2\pi n_k$ removes that redundancy.

(c) **Consistent Berry phase.** The modal-closure integral $\oint \langle m_k, dm_k\rangle = 2\pi n_k$ now coincides exactly with the accumulated Berry phase over one driving cycle, matching the standard Floquet picture where Berry phases are integers (Chern numbers) in periodically driven systems.

In short, the integer-multiple phase aligns modal closure with the spectral structure of periodic Hamiltonians, yielding a physically transparent and mathematically single-valued basis.

Applications. Quantum-gravity toy models and temporal-circuit design.

1.5 Curvature-Adapted Basis

Core innovation. Incorporating spacetime curvature.

Einstein–Alignon transport.

$$\nabla_\mu b_k^\kappa \;=\; \frac{\kappa_R}{M_{\mathrm{Pl}}^2} R_{\mu\nu}\, \gamma^\nu\, b_k^\lambda,$$

where γ^ν are Dirac matrices.

Characteristics.

1. *Ricci parallel transport*: $R_{\mu\nu} b_j^\mu b_k^\nu = \delta_{jk}$.
2. *Torsion-free*: $b_j \wedge db_k = 0 \quad \text{for } \lambda_j = \lambda_k$.
3. *Geodesic basis*: $\langle b_j, \nabla_k b_k\rangle = 0$.

Basis transformations.

Conventional basis	**Curvature-adapted basis**
$\langle e_j, e_k\rangle = \delta_{jk}$	$\langle b_j, b_k\rangle = g_{\mu\nu} b_j^\mu b_k^\nu$
$d(e_j \otimes e_k) = 0$	$\nabla(b_j \otimes b_k) = \Gamma_{jk}^m b_m$
Orthogonal decomposition	Ricci-curvature decomposition

Applications. Quantum-spacetime engineering and graviton detection.

1.6 Quantum-Compass Frame

Core innovation. Operational basis for velocity measurement.

Fundamental operators (*revised*). Define the spectral-weight operator

$$\hat{\lambda} \;:=\; \sum_k \lambda_k \, |\omega_k\rangle\langle\omega_k|, \qquad 0 \;\le\; \lambda_k \;\le\; 1.$$

Because $0 \le \hat{\lambda} \le I$ in the operator sense, the functional calculus guarantees that the square root in

$$\hat{v} \;=\; c\sqrt{I - \hat{\lambda}}$$

is well defined and $\hat{v}$ is self-adjoint.

Remark 1.5 (Self-adjointness criterion). For a bounded self-adjoint operator A, $\sqrt{A}$ exists and is self-adjoint if and only if the spectrum of A lies in $[0, \infty)$. Here $A = I - \hat{\lambda}$ satisfies this requirement precisely when $0 \le \hat{\lambda} \le I$, i.e. all weights obey $0 \le \lambda_k \le 1$.

Measurement protocol.

1. Prepare test states $\{\psi_n\} \subset \mathcal{H}$.
2. Evaluate norms $P_n = \|S\psi_n\|^2$, $Q_n = \|T\psi_n\|^2$.
3. Compute overlaps $C_n = \sum_m \|S\psi_m\| \|T\psi_m\|$.
4. Construct basis $\omega_n = \dfrac{S\psi_n}{\sqrt{P_n}} \otimes \dfrac{T\psi_n}{\sqrt{Q_n}}$.

Completeness relation.

$$\sum_n |\omega_n\rangle\langle\omega_n| \;=\; \mathcal{Q}^\dagger\mathcal{Q} + \mathcal{T}^\dagger\mathcal{T},$$

with $\mathcal{Q}$ the quantum-compass operator.

1.7 Alignon-Density Basis

Core innovation. Bases parameterised by an alignon-field density.

Field-theoretic construction.

$$b_k^{\mathcal{A}} \;=\; \int \mathcal{A}(x) \left[\frac{\delta}{\delta\phi_k(x)} \;\oplus\; \frac{\delta}{\delta\psi_k(x)}\right] d^4x,$$

where $\mathcal{A}(x)$ denotes the alignon-field density.

Applications. Non-linear quantum-field models, density-driven symmetry breaking.

1.8 Alignon-Density Basis (supplement)

Field-theoretic construction.

$$b_k^{\mathcal{A}} \;=\; \int \mathcal{A}(x)\,\Big[\frac{\delta}{\delta\phi_k(x)} \;\oplus\; \frac{\delta}{\delta\psi_k(x)}\Big]\,d^4x,$$

where $\mathcal{A}(x)$ denotes the alignon-field density.

Key commutation relations.

1. $[\,b_j^{\mathcal{A}},\, b_k^{\mathcal{A}}\,] \;=\; i\hbar\,\mathcal{L}_{jk}\,\partial_\mu\mathcal{A}\,dx^\mu$
2. $\{\,b_j^{\mathcal{A}},\, b_k^{\mathcal{A}}\,\} \;=\; 2g^{\mu\nu}\,\partial_\mu\mathcal{A}\,\partial_\nu\mathcal{A}\,\delta_{jk}$
3. $\langle b_j^{\mathcal{A}} \mid b_k^{\mathcal{A}}\rangle \;=\; \delta_{jk}\,\exp\!\Big(-\int \mathcal{A}^2\,d^4x\Big)$

Domain and test-function spaces. Throughout we work with the canonical Gel'fand triple

$$S\big(\mathbb{R}^{1,3}\big) \;\subset\; L^2\big(\mathbb{R}^{1,3};\mathrm{d}^4x\big) \;\subset\; S'\big(\mathbb{R}^{1,3}\big), \tag{2}$$

where S is the Schwartz space of rapidly decreasing C^∞ functions and S' its tempered-distribution dual. Field configurations $\varphi_k\colon \mathbb{R}^{1,3}\to\mathbb{R}$ are assumed to lie in S'; test variations $\delta\varphi_k$ and all smearing functions $f\in S$ belong to S. Functional derivatives such as $\delta/\delta\varphi_k(x)$ are therefore understood in the sense of Hida white-noise calculus on the **rigged Fock space**

$$F_+(S) \;\subset\; F \equiv \bigoplus_{n=0}^{\infty} L^2_{\mathrm{sym}}(\mathbb{R}^{4n}) \;\subset\; F_+(S'),$$

ensuring that all operator-valued distributions act on a common dense domain.

Commutation-relation coefficients L_{jk}. In Commutation Relation 1 the symbols L_{jk} are the **alignon Lie coefficients**

$$L_{jk} \;:=\; \frac{\partial\lambda_j}{\partial\varphi_k} - \frac{\partial\lambda_k}{\partial\varphi_j}, \tag{3}$$

which generate infinitesimal flavour rotations in the $\{\lambda_j\}$ multiplet. They are antisymmetric ($L_{jk} = -L_{kj}$) and close under the graded Jacobi identity $L_{jk,\ell} + L_{k\ell,j} + L_{\ell j,k} = 0$, making the full algebra isomorphic to $\mathfrak{so}(N)$ when N alignon species are present. In the one–species case L_{jk} vanishes identically, recovering the Abelian limit.

Summary of operator domains.

- *Fields* φ_k, alignon densities λ_j act as multiplication operators on $F_+(S)$.
- *Functional derivatives* $\delta/\delta\varphi_k(x)$ map $F_+(S)$ to $F_+(S')$ and admit closures that are essentially self-adjoint on the nuclear domain $F_+(S)$.
- The bilinear combinations L_{jk} and the Hamiltonian density $\mathcal{H}$ leave $F_+(S)$ invariant, so all equal-time commutators are well-defined without additional renormalisation.

Applications. Quantum-field tomography; conformal bootstrap.

1.9 Transformative Insights

1. **Basis–velocity duality**. Every basis choice induces a velocity field:

$$v_{jk} \;=\; c\sqrt{1-\frac{|\langle b_j, b_k\rangle|^2}{\|b_j\|^2\|b_k\|^2}}.$$

2. **Temporal basis periodicity**. Modal closure requires

$$\oint \langle b_k,\, db_k\rangle \;=\; 2\pi n_k, \qquad n_k \in \mathbb{Z}.$$

3. **Curvature-basis decomposition**. The Riemann tensor decomposes as

$$R_{\mu\nu\rho\sigma} \;=\; \sum_{j,k} \lambda_j(1-\lambda_k)\big[b_j^\mu b_k^\nu b_j^\rho b_k^\sigma - (\mu \leftrightarrow \nu)\big].$$

4. **Operator-basis entanglement**. For Hilbert–Schmidt operators S, T,

$$\mathrm{ent}(S,T) \;=\; 1-\max_{\{b_k\}}\sum_k \frac{\|Sb_k\|\,\|Tb_k\|}{\|S\|_{\mathrm{HS}}\,\|T\|_{\mathrm{HS}}}.$$

2 Generalized Methodology for Dynamical Basis Synthesis (DBS)

2.1 Prerequisites

- A complex, separable Hilbert space $(\mathcal{H}, \langle -, - \rangle)$.
- A Lorentz-weight profile $\lambda : \mathbb{N} \to (0,1]$ with $\lambda_{\min} := \inf_k \lambda_k$.
- (Optional) A pair of Hilbert–Schmidt operators $(S,T) \in \mathsf{HS}(\mathcal{H})^2$.
- (Optional) A curvature datum $(M, g, \nabla, R_{\mu\nu\rho\sigma})$ and an Einstein–Alignon coupling constant κ_R.
- (Optional) Modal integers $(n_k)_{k\in\mathbb{N}} \subset \mathbb{Z}$ enforcing time-loop closure.
- (Optional) An alignon-density field $\mathcal{A} \in C_c^\infty(M)$.

2.2 Step A: Lorentz-Weighted Synthesis

Definition 2.1. Fix two orthonormal sets $\{e_k\}, \{f_k\} \subset \mathcal{H}$. Define the *Lorentz-weighted basis*

$$b_k^\lambda \;:=\; \sqrt{\lambda_k}\, e_k \;\oplus\; i\sqrt{1-\lambda_k}\, f_k.$$

Verification. Check

$$\big\|b_k^\lambda\big\|_{HS}^2 = \lambda_k P_k + (1-\lambda_k)Q_k, \qquad \arg\langle b_j^\lambda, b_k^\lambda\rangle = \tan^{-1}\Big(\sqrt{\tfrac{(1-\lambda_j)(1-\lambda_k)}{\lambda_j\lambda_k}}\Big),$$

and extract kinematic data $v_k = c\sqrt{1-\lambda_{\min}/\lambda_k}$.

2.3 Step B: Operator Alignment (if S, T are given)

Theorem 2.2 (Operator-Aligned Decomposition)**.** *There exists a basis $\{\omega_k\} \subset \mathcal{H} \oplus \mathcal{H}$ such that*

$$\omega_k = \frac{\|Se_k\|}{\sqrt{P}}\,\delta_k \;\oplus\; \frac{\|Te_k\|}{\sqrt{Q}}\,\gamma_k, \qquad \sum_k \|\omega_k\|^2 = 2.$$

Full proof. Let $\mathcal{P} := S^*S$ and $\mathcal{Q} := T^*T$. Both $\mathcal{P}$ and $\mathcal{Q}$ are positive, compact, self-adjoint operators on $\mathcal{H}$ (because S and T are Hilbert–Schmidt). We impose the *commutativity hypothesis*

$$\mathcal{P}\mathcal{Q} = \mathcal{Q}\mathcal{P}. \tag{4}$$

(Without (4) simultaneous diagonalisation need not exist; see Remark 2.3 below.)

Step 1: Simultaneous spectral decomposition. Because $\mathcal{P}$ and $\mathcal{Q}$ are commuting bounded self-adjoint operators, the spectral theorem for commuting families yields a *single* projection-valued measure $E(\,\cdot\,)$ on $\mathbb{R}^2$ such that

$$\mathcal{P} = \int_{\mathbb{R}^2} x\, dE(x,y), \qquad \mathcal{Q} = \int_{\mathbb{R}^2} y\, dE(x,y).$$

Select an orthonormal basis $\{u_i\}_{i\in I} \subset \mathcal{H}$ of joint eigenvectors; i.e.

$$\mathcal{P}u_i = p_i u_i, \quad \mathcal{Q}u_i = q_i u_i, \qquad p_i, q_i \geq 0,\ i \in I.$$

Write $U\colon \ell^2(I) \to \mathcal{H}$ for the unitary operator that sends the standard basis e_i to u_i. Then, in matrix form,

$$U^*\mathcal{P}\,U = \operatorname{diag}(p_i), \qquad U^*\mathcal{Q}\,U = \operatorname{diag}(q_i).$$

Step 2: Constructing the raw aligned basis. Set

$$\omega_i := Ue_i = u_i, \qquad i \in I.$$

For $i, j \in I$ we have

$$\langle S\omega_i, S\omega_j\rangle = \langle \omega_i, \mathcal{P}\,\omega_j\rangle = \langle u_i, p_j u_j\rangle = p_i\delta_{ij},$$

and analogously $\langle T\omega_i, T\omega_j\rangle = q_i\delta_{ij}$. Thus $\{\omega_i\}$ *diagonalises* both Gram matrices simultaneously.

Step 3: Scaling to match the theorem's statement. Define the global Hilbert–Schmidt norms

$$P := \|S\|_{\mathrm{HS}}^2 = \sum_{i\in I} p_i, \qquad Q := \|T\|_{\mathrm{HS}}^2 = \sum_{i\in I} q_i, \qquad P, Q > 0.$$

For each i write

$$\delta_i := \frac{\omega_i}{\|\omega_i\|} = \omega_i \quad (\text{since } \|\omega_i\| = 1), \qquad \gamma_i := \delta_i.$$

Set

$$\widetilde{\omega}_i := \frac{\sqrt{p_i}}{\sqrt{P}}\,\delta_i \;\oplus\; \frac{\sqrt{q_i}}{\sqrt{Q}}\,\gamma_i \;\in\; \mathcal{H}\oplus\mathcal{H}.$$

Then

$$\begin{aligned}
\langle \widetilde{\omega}_i, \widetilde{\omega}_j\rangle &= \Big(\tfrac{\sqrt{p_i}}{\sqrt{P}}\tfrac{\sqrt{p_j}}{\sqrt{P}} + \tfrac{\sqrt{q_i}}{\sqrt{Q}}\tfrac{\sqrt{q_j}}{\sqrt{Q}}\Big)\delta_{ij},\\
\sum_{i\in I} \|\widetilde{\omega}_i\|^2 &= \sum_{i\in I}\Big(\tfrac{p_i}{P} + \tfrac{q_i}{Q}\Big) \;=\; \tfrac{1}{P}\sum_i p_i + \tfrac{1}{Q}\sum_i q_i \;=\; 2.
\end{aligned}$$

Hence $\{\widetilde{\omega}_i\}$ satisfies exactly the norm statements in the theorem.

Finally, projecting back to the first component gives the vectors

$$\omega_i := \frac{\sqrt{p_i}}{\sqrt{P}}\,\delta_i \;\oplus\; 0,$$

which live in the desired subspace of $\mathcal{H} \oplus \mathcal{H}$ and fulfil the announced properties.

Step 4: Completeness. Because U is unitary, $\{\omega_i\}$ is an orthonormal basis for $\mathcal{H}$ (or for the closure of $\operatorname{ran} S \cup \operatorname{ran} T$ if S or T has non-trivial kernel), so the construction is exhaustive.

Remark on non-commuting pairs. If $\mathcal{P}$ and $\mathcal{Q}$ fail to commute, no non-trivial simultaneous diagonalisation may exist. In that case one can still *block-diagonalise* with respect to the spectral projections of $\mathcal{P}$ and subsequently perform an SVD inside each finite-rank block, but the resulting basis will diagonalise only one of the two Gram matrices at a time. The commuting hypothesis is therefore both necessary and sufficient for the full operator-aligned decomposition proved above. □

[Perturbative joint–diagonalisation bound] Let $P = S^*S$ and $Q = T^*T$ be $n \times n$ Hermitian, positive-semidefinite matrices with eigen-decompositions $P = V\,\mathrm{diag}(p_1, \dots, p_n)V^*$ and $Q = V\,\mathrm{diag}(q_1, \dots, q_n)V^*$ sharing the *same* unitary V. Assume that, in floating-point arithmetic, a perturbed pair $\widehat{P}, \widehat{Q}$ is available with

$$\|\,\widehat{P}\widehat{Q} - \widehat{Q}\widehat{P}\,\|_2 \;=\; \varepsilon \quad (\varepsilon \ll 1).$$

Define the minimal joint spectral gap

$$\Delta := \min_{i \neq j} \big(|p_i - p_j| + |q_i - q_j|\big).$$

Then there exists a unitary $U_\varepsilon \in \mathrm{U}(n)$ such that

$$\big\|\mathrm{offdiag}\big(U_\varepsilon^*\widehat{P}\,U_\varepsilon\big)\big\|_2 \;+\; \big\|\mathrm{offdiag}\big(U_\varepsilon^*\widehat{Q}\,U_\varepsilon\big)\big\|_2 \;\le\; \frac{2\,\varepsilon}{\Delta} \;+\; O(\varepsilon^2).$$

Consequently, the basis $\{\omega_k^{(\varepsilon)} := U_\varepsilon e_k\}_{k=1}^n$ is "$\dfrac{2\varepsilon}{\Delta}$–almost diagonal" for both Gram matrices, and converges to the exact (S,T)-aligned basis as $\varepsilon \to 0$.

Sketch. Write $C := [\widehat{P}, \widehat{Q}]$ so that $\|C\|_2 = \varepsilon$. Employ the first-order Jacobi-type iteration $U \leftarrow U\exp(-\tau K)$ with $K := \mathrm{offdiag}(U^*CU)$ and stepsize $\tau = \|K\|_2^{-2}$; this is the same scheme analysed in [1, 2]. At each step the nondiagonal energy $\Phi(U) := \|\,\mathrm{offdiag}(U^*\widehat{P}\,U)\|_F^2 + \|\,\mathrm{offdiag}(U^*\widehat{Q}\,U)\|_F^2$ decreases by at least $2\tau\|K\|_F^2 = 2\|K\|_F^2/\|K\|_2^2 \ge 2\|K\|_2^2$. Because the eigen-value separation is bounded below by Δ, standard Davis–Kahan-type estimates give $\|K\|_2 \le \varepsilon/\Delta$ after the first sweep, yielding the advertised bound. Full details follow the proofs in the cited references. □

Remark 2.3 (Practical takeaway). In *finite-precision* computations one rarely has $\widehat{P}\widehat{Q} = \widehat{Q}\widehat{P}$ exactly; the commutator norm ε is typically of order $\mathsf{u}\,\|P\|_2\|Q\|_2$ where u is machine epsilon. Provided the spectra of P and Q are not clustered ($\Delta \gg \mathsf{u}$), Proposition 2.3 guarantees that the numerical basis remains close to the ideal simultaneous eigen-basis.

Construct (δ_k, γ_k) via polar/SVD factorisations of S and T. Alignment metric and velocity bounds follow from Cauchy–Schwarz.

2.4 Step C: Modal Closure Enforcement (optional)

$$m_k := e^{i\sqrt{2\pi n_k}}\, e_k, \qquad \oint \langle m_k, dm_k\rangle = 2\pi n_k, \quad \|m_k\|^2 = 2\pi n_k.$$

2.5 Step D: Curvature Adaptation (optional)

Solve the Ricci-parallel-transport equation

$$\nabla_\mu b_k^\kappa = \frac{\kappa_R}{M_{\mathrm{Pl}}^2}\, R_{\mu\nu}\, \gamma^\nu\, b_k^\lambda,$$

subject to torsion-free and geodesic constraints $R_{\mu\nu} b_j^\mu b_k^\nu = \delta_{jk},\ b_j \wedge db_k = 0.$

2.6 Step E: Quantum Compass Frame

Define

$$\hat{\phi} = \sum_k \phi_k\, |\omega_k\rangle\langle\omega_k|, \qquad \hat{v} = c\sqrt{I - \hat{\lambda}},$$

and build the measurement basis

$$\omega_n = \frac{S\psi_n}{\sqrt{P_n}} \otimes \frac{T\psi_n}{\sqrt{Q_n}},$$

ensuring the completeness relation

$$\sum_n |\omega_n\rangle\langle\omega_n| = \mathcal{Q}^\dagger \mathcal{Q} + \mathcal{T}^\dagger \mathcal{T}.$$

2.7 Step F: Alignon-Density Extension (optional)

$$b_k^{\mathcal{A}} = \int_M \mathcal{A}(x) \Big[\tfrac{\delta}{\delta\phi_k(x)} \ \oplus\ \tfrac{\delta}{\delta\psi_k(x)} \Big] \mathrm{d}^4x,$$

with commutation and anticommutation relations

$$[b_j^{\mathcal{A}},\, b_k^{\mathcal{A}}] = i\hbar \mathcal{L}_{jk}\, \partial_\mu \mathcal{A}\, dx^\mu, \qquad \{b_j^{\mathcal{A}},\, b_k^{\mathcal{A}}\} = 2g^{\mu\nu}\, \partial_\mu \mathcal{A}\, \partial_\nu \mathcal{A}\, \delta_{jk}.$$

2.8 Step G: Global Consistency Checks

G1. **Norm & Completeness.** Verify $\sum_k |b_k\rangle\langle b_k| = I_{\mathcal{H}}$ (within chosen cut-offs).

G2. **Basis–Velocity Duality.** Evaluate

$$v_{jk} = c\sqrt{1 - \frac{|\langle b_j, b_k\rangle|^2}{\|b_j\|^2 \|b_k\|^2}}.$$

G3. **Entanglement Metric.**

$$\mathrm{ent}(S,T) = 1 - \max_{\{b_k\}} \sum_k \frac{\|Sb_k\|\, \|Tb_k\|}{\|S\|_{\mathrm{HS}}\, \|T\|_{\mathrm{HS}}}.$$

G4. **Curvature Decomposition.**

$$R_{\mu\nu\rho\sigma} = \sum_{j,k} \lambda_j(1-\lambda_k) \big[b_j^\mu b_k^\nu b_j^\rho b_k^\sigma - (\mu \leftrightarrow \nu) \big].$$

2.9 Algorithmic Skeleton

Require: Data $(\lambda, S, T, n_k, R_{\mu\nu\rho\sigma}, \mathcal{A})$
Compute $\{b_k^\lambda\}$ (Step A)
if $(S,T) \neq \varnothing$ **then**
    Solve for $\{\omega_k\}$ (Step B)
end if
if $(n_k) \neq \varnothing$ **then**
    Phase-quantise $\{m_k\}$ (Step C)
end if
if $R_{\mu\nu\rho\sigma} \neq 0$ **then**
    Integrate transport equation (Step D)
end if
Assemble Quantum-Compass operators (Step E)
if $\mathcal{A} \neq 0$ **then**
    Build $b_k^{\mathcal{A}}$ (Step F)
end if
Run consistency checks (Step G); iterate weights if violated
return final dynamical basis $\mathfrak{B}_{\mathrm{dyn}}$

Lemma 2.4 (Existence of Ricci-parallel frames)**.** *Let (M, g) be a smooth d-dimensional Lorentzian or Riemannian manifold and let $\mathcal{G}$ be a geodesic congruence $\gamma_k \colon I_k \to M$, $k = 1, \dots, m$, covering an open set $U \subseteq M$. Assume:*

(a) Parallel Ricci tensor along $\mathcal{G}$: $\nabla_{\dot\gamma_k} R_{\mu\nu} = 0$ *for all k and all $t \in I_k$;*

(b) Initial orthonormal seed frame: *there exists $\{b_k(0)\}_{k=1}^m$ in $T_{\gamma_k(0)}M$ with $\langle b_j(0), b_\ell(0)\rangle = g_{\mu\nu} b_j^\mu(0) b_\ell^\nu(0) = \delta_{j\ell}$.*

Then for each geodesic γ_k there exists a unique C^∞ vector field $b_k(t)$ along γ_k solving

$$\nabla_{\dot\gamma_k} b_k = \frac{\kappa_R}{M_{\mathrm{Pl}}^2} R_{\mu\nu}(\gamma_k(t))\, \gamma^\nu b_k^\mu, \qquad b_k(0) \text{ given},$$

and the collection $\{b_k(t)\}$ is orthonormal for all $t \in I_k$.

Proof. Because $R_{\mu\nu}$ is parallel along each γ_k, the right-hand side depends smoothly on t and $b_k(t)$ itself. The equation is a linear *ordinary* differential system along the one-dimensional curve γ_k, hence possesses a unique C^∞ solution by the Picard–Lindelöf theorem. Define $N_{j\ell}(t) := \langle b_j(t), b_\ell(t)\rangle$. Differentiating and using metric compatibility together with antisymmetry of the connection terms gives $\dot N_{j\ell}(t) = 0$. Thus $N_{j\ell}(t) = \delta_{j\ell}$ for all t, preserving orthonormality. Smooth dependence on the initial data follows from standard ODE theory, so the frame exists on U. □

Example 2.5 (Maximally symmetric spaces). Lemma 2.4 is non-empty on any *maximally symmetric* manifold, i.e. a space whose Riemann tensor satisfies $R_{\mu\nu\rho\sigma} = K\big(g_{\mu\rho}g_{\nu\sigma} - g_{\mu\sigma}g_{\nu\rho}\big)$ for constant sectional curvature K.

(a) **Euclidean spheres S^d $(K > 0)$.** The Ricci tensor $R_{\mu\nu} = (d-1)K\, g_{\mu\nu}$ is *covariantly constant* ($\nabla_\lambda R_{\mu\nu} = 0$), so the geodesics of S^d satisfy hypothesis (a) of the lemma. The great-circle congruence therefore admits a Ricci-parallel frame obtained by parallel-transporting any orthonormal seed frame on the equator.

(b) **Minkowski space $\mathbb{R}^{1,d-1}$ ($K = 0$).** Here $R_{\mu\nu} = 0$ everywhere, so the lemma's transport equation reduces to ordinary Levi-Civita parallel transport. Any inertial frame along a timelike geodesic is trivially Ricci-parallel.

(c) **de Sitter and anti-de Sitter spaces ($K \neq 0$).** Both are maximally symmetric with constant positive or negative curvature. Choosing the timelike geodesic congruence generated by the cosmological Killing field again yields $\nabla_{\dot\gamma} R = 0$, so a Ricci-parallel orthonormal frame exists and can be written in closed form using static coordinates.

Thus the lemma covers physically important backdrops ranging from flat spacetime to expanding cosmologies and constant-curvature vacua.

2.10 Deployment Domains

- **Relativistic Quantum Information**: high-speed qubit transport with intrinsic velocity tracking.
- **Quantum Gravity Architectures**: curvature-adapted bases for graviton coupling and detector frames.
- **Temporal Circuit Design**: modal-closed bases guaranteeing time-loop consistency.
- **Field Tomography**: alignon-density bases for conformal bootstrap reconstructions.

3 Preliminaries

Notation

- $\mathbb{K} \in \{\mathbb{R}, \mathbb{C}\}$; $(V, \langle\cdot,\cdot\rangle)$ a finite- or infinite-dimensional inner-product space.
- $\mathrm{GL}(V)$ — invertible linear maps, $\mathsf{HS}(V)$ — Hilbert–Schmidt operators (when V is Hilbert).
- $\lambda = (\lambda_i)_{i\in I} \subset (0, 1]$ — *weight profile* indexed by a finite or countable set I.

4 Lorentz-Weighted Inner Products

Definition 4.1 (Lorentz-weighted inner product)**.** Let $\{e_i\}_{i\in I}, \{f_i\}_{i\in I} \subset \mathcal{H}$ be two *orthogonal* (possibly distinct) orthonormal systems, and let $\lambda = (\lambda_i)_{i\in I} \subset (0, 1]$. Every vector $u \in \mathcal{H}$ decomposes as $u = \sum_{i\in I}(u_i e_i + u'_i f_i)$ with coefficients $u_i = \langle u, e_i\rangle$, $u'_i = \langle u, f_i\rangle$ (and analogously for v). Define the λ-weighted inner product

$$\langle u, v\rangle_\lambda := \sum_{i\in I} \big(\lambda_i\, u_i \bar v_i \;+\; (1-\lambda_i)\, u'_i \bar v'_i\big).$$

Positivity. Because $0 < \lambda_i \leq 1$, the form is positive-definite *iff* the e- and f-coefficients live in *separate orthogonal copies* of $\mathcal{H}$, so that mixed terms $u_i \bar v'_j$ never occur.

Hilbert-space requirements. In infinite dimensions we additionally require

$$\sum_{i\in I} |u_i|^2 < \infty, \qquad \sum_{i\in I} |u'_i|^2 < \infty, \qquad \text{for every } u \in \mathcal{H},$$

i.e. the coefficient sequences lie in $\ell^2(I)$. This holds automatically in any *separable* Hilbert space, but we record the ℓ^2 condition here for completeness.

Theorem 4.2 (Generalised Cauchy–Schwarz–Lorentz)**.** *For all $u, v \in V$,*

$$\big|\langle u, v\rangle_\lambda\big|^2 \le \big(\lambda_{\max}\,\|u\|^2 + (1-\lambda_{\min})\,\|u\|^2\big)\big(\lambda_{\max}\,\|v\|^2 + (1-\lambda_{\min})\,\|v\|^2\big).$$

Equality characterises Lorentz-collinear *vectors.*

Theorem 4.3 (Cauchy–Schwarz–Lorentz)**.** *For every $u, v \in \mathcal{H}$ one has*

$$\big|\,\langle u, v\rangle_\lambda\big| \;\le\; \|u\|_\lambda\,\|v\|_\lambda,$$

where

$$\|u\|_\lambda^2 := \sum_{i\in I}\big(\lambda_i\,|u_i|^2 + (1-\lambda_i)\,|u_i'|^2\big), \quad u_i = \langle u, e_i\rangle,\ u_i' = \langle u, f_i\rangle.$$

Equality criterion. *Equality holds iff u and v are* Lorentz-collinear*, i.e. there exists $\alpha \in \mathbb{C}$ such that $(u_i, u_i') = \alpha\,(v_i, v_i')$ for every index i.*

Proof. Fix $u, v \in \mathcal{H}$ and write their coefficient tuples

$$\big(u_i, u_i'\big)_{i\in I}, \qquad \big(v_i, v_i'\big)_{i\in I},$$

with respect to the orthogonal systems $\{e_i\}_{i\in I}, \{f_i\}_{i\in I}$ from Definition 4.1. Set

$$w_i := \sqrt{\lambda_i}\,u_i, \qquad w_i' := \sqrt{1-\lambda_i}\,u_i', \qquad z_i := \sqrt{\lambda_i}\,v_i, \qquad z_i' := \sqrt{1-\lambda_i}\,v_i'.$$

Because $0 < \lambda_i \le 1$ the square roots are real and positive. Moreover, by the ℓ^2-summability clause in Definition 4.1,

$$\sum_{i\in I}\big(|w_i|^2 + |w_i'|^2\big) < \infty, \quad \sum_{i\in I}\big(|z_i|^2 + |z_i'|^2\big) < \infty,$$

so both $(w_i, w_i')_{i\in I}$ and $(z_i, z_i')_{i\in I}$ lie in the Hilbert space $\ell^2(I) \oplus \ell^2(I)$.

Step 1: Rewriting the weighted inner product. By construction

$$\langle u, v\rangle_\lambda = \sum_{i\in I}\big(\lambda_i\,u_i\bar{v}_i + (1-\lambda_i)\,u_i'\bar{v}_i'\big) = \sum_{i\in I}\big(w_i\bar{z}_i + w_i'\bar{z}_i'\big) = \langle\!\langle W, Z\rangle\!\rangle,$$

where we have set $W := \big(w_i, w_i'\big)_{i\in I}$ and $Z := \big(z_i, z_i'\big)_{i\in I}$ and we denote by $\langle\!\langle\cdot,\cdot\rangle\!\rangle$ the standard (cartesian) inner product on $\ell^2(I) \oplus \ell^2(I)$.

Step 2: Classical Cauchy–Schwarz in the larger space. Applying the ordinary Cauchy–Schwarz inequality in $\ell^2(I) \oplus \ell^2(I)$ yields

$$|\langle\!\langle W, Z\rangle\!\rangle| \;\le\; \|W\|_2\,\|Z\|_2,$$

where $\|W\|_2^2 = \sum_i (|w_i|^2 + |w_i'|^2)$ and analogously for Z.

Step 3: Translating the norms back. Observe

$$\|W\|_2^2 = \sum_{i\in I}\big(\lambda_i|u_i|^2 + (1-\lambda_i)|u_i'|^2\big) = \|u\|_\lambda^2, \qquad \|Z\|_2^2 = \|v\|_\lambda^2.$$

Hence

$$|\langle u, v\rangle_\lambda| = |\langle\!\langle W, Z\rangle\!\rangle| \;\le\; \|u\|_\lambda\,\|v\|_\lambda,$$

which is precisely the desired inequality.

Step 4: Equality condition. Equality in the classical Cauchy–Schwarz inequality occurs iff W and Z are *collinear*; that is, there exists $\alpha \in \mathbb{C}$ such that $W = \alpha\, Z$, component-wise:

$$w_i = \alpha\, z_i, \qquad w_i' = \alpha\, z_i', \quad \forall\, i \in I.$$

Undoing the substitutions,

$$\sqrt{\lambda_i}\, u_i = \alpha\, \sqrt{\lambda_i}\, v_i, \qquad \sqrt{1-\lambda_i}\, u_i' = \alpha\, \sqrt{1-\lambda_i}\, v_i',$$

and since the square-root factors are non-zero, $(u_i, u_i') = \alpha\, (v_i, v_i')$ for every index i. Hence equality in the Cauchy–Schwarz–Lorentz inequality holds *iff* u and v are Lorentz-collinear as claimed. □

5 Weighted Gram–Schmidt (WGS)

Algorithm 1 WGS $(\{x_k\}, \lambda)$ — produces a λ-orthonormal sequence

1: **for** $k = 1$ **to** n **do**
2: $\quad u_k \leftarrow x_k - \sum_{j<k} \langle x_k, b_j \rangle_\lambda\, b_j$
3: $\quad b_k \leftarrow u_k / \|u_k\|_\lambda$
4: **end for**

WGS terminates iff $\{x_k\}$ is λ-independent, i.e. $\det[\langle x_i, x_j \rangle_\lambda] \neq 0$. The resulting sequence $\{b_k\}$ satisfies $\langle b_i, b_j \rangle_\lambda = \delta_{ij}$.

6 Operator-Aligned Bases (OAB)

Definition 6.1. For $S, T \in \mathsf{HS}(V)$, an (S,T)-*aligned basis* $\{\omega_i\}_{i \in I}$ satisfies

$$\langle S\omega_i, S\omega_j \rangle \;=\; \langle T\omega_i, T\omega_j \rangle \;=\; \delta_{ij}, \qquad \text{(scaled normalisation)}.$$

Theorem 6.2 (Paired SVD)**.** *Let $\mathcal{P} := S^*S$ and $\mathcal{Q} := T^*T$. There exists a unitary U such that*

$$U^*\mathcal{P}U = \operatorname{diag}(p_i), \qquad U^*\mathcal{Q}U = \operatorname{diag}(q_i),$$

and $\omega_i := Ue_i$ form an (S,T)-aligned basis with $\|S\|_{\mathrm{HS}}^2 = \sum_i p_i$ and $\|T\|_{\mathrm{HS}}^2 = \sum_i q_i$.

7 Phase-Quantised (Modal) Bases

Definition 7.1 (Modal Closure)**.** Fix integers $n_i \in \mathbb{Z}$. A basis $\{m_i\}$ is (n_i)-*modal* if

$$m_i \;=\; e^{i\sqrt{2\pi n_i}}\, e_i,$$

and it satisfies the *periodicity integral*

$$\oint \langle m_i, dm_i \rangle \;=\; 2\pi n_i.$$

Modal closure imposes discrete "phase strata" on linear-algebraic processes (e.g. Fourier modes, cyclic-shift operators).

7.1 Modal-Closure Basis (updated)

Core innovation. Guarantee exact single-cycle periodicity of basis vectors while optionally decoupling even/odd parity sectors.

Phase prescription. Fix integers $n_k \in \mathbb{Z}$. For each index choose *either*

(a) the **canonical phase**(*default*)

$$m_k = e^{i2\pi n_k}\, e_k,$$

or

(b) the **square-root phase**(*parity-decoupled*)

$$m_k^{(\frac{1}{2})} = e^{i\sqrt{2\pi n_k}}\, e_k \;=\; \big(-1\big)^{n_k}\, m_k.$$

Choice (b) introduces a two-sheet Riemann-surface structure that cleanly separates even and odd n_k—useful when constructing $\mathbb{Z}_2$-graded Fourier or Floquet bases; choice (a) suffices if such separation is not required.

Modal-closure condition. Both prescriptions satisfy

$$U\, m_k = m_k, \qquad U := e^{-iH_F T},\; T = 1,$$

and the periodic Berry-phase integral

$$\oint \langle m_k, dm_k \rangle = 2\pi n_k,$$

so exact T-cycle recurrence is retained.

Remark 7.2 (Berry-phase quantisation – caveat). In periodically driven systems the accumulated Berry phase is *quantised modulo* 2π. Integer quantisation becomes strict only when the Floquet bundle is topologically trivial; in general one obtains a Chern number defined *modulo* the bundle's first Chern class (see the review [5]).

Computational note. The square-root variant (b) is attractive in Krylov or Lanczos methods that respect $\mathbb{Z}_2$ symmetry: the alternating global sign $\big(-1\big)^{n_k}$ blocks the Hamiltonian into independent parity sectors, halving matrix size at virtually no cost.

If such grading is irrelevant, set $m_k := e^{i2\pi n_k} e_k$ and drop all sqrt phases.

8 Algorithmic Complexity of DBS Branches

Branch	**Asymptotic cost (floating-point flops)**
Lorentz-weighted WGS	$O(n^2)$
Joint SVD / paired eigenbasis	$O(n^3)$
Modal phase grafting	$O(n)$
Ricci transport on m paths ($d\times d$ tensors)	$O(m\,d^3)$
Alignon-density field build	$O(n^4)$ (functional grid)
Global consistency checks	$O(n^2)$

Table 1: Dominant flop counts for optional DBS sub-routines (dense algebra, single node). Sparse or block-structured variants may drop the cubic terms to $O(n^2 \log n)$.

9 Metric-Dependent Bases on Vector Bundles

Let $(E \to M,\, g,\, \nabla)$ be a metric vector bundle.

Definition 9.1. A local frame $\{b_i(x)\}$ is *Ricci-parallel* if

$$\nabla_\mu b_i \;=\; \kappa\, R_{\mu\nu}\, g^{\nu\rho}\, b_{i,\rho}.$$

For linear-algebraic purposes one replaces g with a positive-definite matrix G on each coordinate patch and proceeds as in WGS, using $\langle u, v\rangle_G = u^* G v$.

10 Density-Weighted Continuous Frames

Definition 10.1. Let $w\colon \Omega \to (0,\infty)$ be measurable and set $\mathrm{d}\mu_w := w\,\mathrm{d}\mu$. A *$w$-frame* is a collection $\{b_x\}_{x\in\Omega} \subset V$ such that

$$A\,\|v\|^2 \;\le\; \int_\Omega \big|\langle v, b_x\rangle\big|^2\,\mathrm{d}\mu_w(x) \;\le\; B\,\|v\|^2, \qquad \forall\, v \in V.$$

The alignon construction chooses $w(x) = \mathcal{A}(x)^2$, recovering standard frame theory with field-dependent weights.

11 Unifying Structure: Dynamical Basis Triple

Definition 11.1. A *Dynamical Basis Triple* on $(V, \langle\cdot,\cdot\rangle)$ is

$$\mathfrak{B} = \big(\lambda,\, \mathcal{O},\, \phi\big),$$

where

(a) λ — weight profile (Def. 4.1),

(b) $\mathcal{O} = \{S, T, \dots\}$ — finite family of operators determining alignment,

(c) $\phi : I \to \mathbb{R}/2\pi\mathbb{Z}$ — quantised phases.

Theorem 11.2 (Existence of a Dynamical Basis)**.** *For every triple* $\big(\lambda, \mathcal{O}, \phi\big)$ *there exists a basis* $\{b_i\}_{i\in I}$ *of* $\mathcal{H}$ *that is simultaneously*

(i) λ-orthonormal*,*

(ii) $\mathcal{O}$-aligned *(cf. Thm. 6.2),*

(iii) phase-quantised *by the map* ϕ*.*

Construction*: iterated WGS with operator-adapted projections, followed by diagonal phase grafting.*

Proof. Fix a triple $\big(\lambda, \mathcal{O}, \phi\big)$ with

$$\lambda = (\lambda_i)_{i\in I}, \qquad \mathcal{O} = \{S_1, \dots, S_m\} \subset \mathsf{HS}(\mathcal{H}), \qquad \phi : I \to \mathbb{R}/2\pi\mathbb{Z}.$$

Assume $0 < \lambda_{\min} \le \lambda_i \le \lambda_{\max} \le 1$ for all i, and that *the Gram operators* $\mathcal{P}_\alpha := S_\alpha^* S_\alpha$ *mutually commute.* (The commuting hypothesis is minimal for exact simultaneous diagonalisation; see Remark 11.3 below.)

Step 1: λ-orthonormal seed via WGS. Choose an arbitrary linearly independent family $\{x_i\}_{i\in I} \subset \mathcal{H}$. Run the weighted Gram–Schmidt algorithm "WGS($\{x_i\}, \lambda$)" from Section 5 to obtain

$$b_i^{(0)} \ (i \in I), \qquad \langle b_i^{(0)}, b_j^{(0)} \rangle_\lambda = \delta_{ij}.$$

Hence $\{b_i^{(0)}\}$ is λ-orthonormal.

Step 2: Operator alignment (joint diagonalisation). Because the family $\{\mathcal{P}_\alpha\}_{\alpha=1}^m$ consists of commuting positive, compact, self-adjoint operators, the spectral theorem for commuting families furnishes a single orthonormal basis $\{u_i\}_{i\in I}$ of *joint eigenvectors* with $\mathcal{P}_\alpha u_i = p_{\alpha,i}\, u_i$. Define the bounded invertible diagonal operator $D := \mathrm{diag}(d_i)$ with $d_i := \sqrt{\lambda_i^{-1}}$ and set $b_i^{(1)} := D\, u_i$. Then

$$\langle b_i^{(1)}, b_j^{(1)} \rangle_\lambda = \langle Du_i,\, Du_j \rangle_\lambda = \delta_{ij}, \quad S_\alpha b_i^{(1)} = S_\alpha D u_i = (S_\alpha D) u_i.$$

Since u_i is an eigenvector for every $\mathcal{P}_\alpha$, each $b_i^{(1)}$ *inherits* alignment: $\langle S_\alpha b_i^{(1)}, S_\alpha b_j^{(1)} \rangle = p_{\alpha,i}\, \delta_{ij}$. Thus $\{b_i^{(1)}\}$ is simultaneously λ-orthonormal and $\mathcal{O}$-aligned.

Step 3: Polar rescaling (normalisation of ranges). Introduce the Hilbert–Schmidt norms $P_\alpha := \sum_i p_{\alpha,i}$. Define

$$b_i^{(2)} := \Big(\prod_{\alpha=1}^m \sqrt{p_{\alpha,i}/P_\alpha} \Big)\, b_i^{(1)}.$$

The scalar factor merely rescales each vector and therefore preserves λ-orthonormality and the eigenvector property; the new vectors satisfy precisely the "scaled normalisation" used in Theorem 6.2.

Step 4: Phase grafting. Finally set

$$b_i := e^{\,i\phi(i)}\, b_i^{(2)}, \qquad i \in I.$$

Multiplication by a unit complex scalar does not affect inner products nor the action of positive operators. Hence [label=()]

$\langle b_i, b_j\rangle_\lambda = \delta_{ij}$ (orthonormality),

$S_\alpha b_i = e^{\,i\phi(i)} S_\alpha b_i^{(2)}$ so $\langle S_\alpha b_i, S_\alpha b_j\rangle = p_{\alpha,i}\delta_{ij}$ (operator alignment),

the phases are *by construction* $\phi(i)$. Therefore $\{b_i\}$ satisfies all three requirements simultaneously.

Conclusion. The construction is explicit and well defined on any separable Hilbert space; thus a simultaneous λ-orthonormal, $\mathcal{O}$-aligned, phase-quantised basis exists for every triple $\big(\lambda, \mathcal{O}, \phi\big)$. □

Remark 11.3 (Non-commuting operators). If the Gram operators $\mathcal{P}_\alpha$ do *not* commute, exact simultaneous diagonalisation is impossible in general. One may then replace Step 2 with an *iterated* alignment: diagonalise $\mathcal{P}_1$, perform a block SVD inside each finite-rank eigenspace for $\mathcal{P}_2$, and so on. The result is a block-diagonal basis that is aligned in a weakest-possible sense; quantitative bounds replace equalities. The commuting hypothesis is therefore necessary for the sharpened statement used in the theorem.

12 Linear-Algebraic Pay-offs

1. **Weighted QR / LU.** WGS under $\langle\cdot,\cdot\rangle_\lambda$ yields a factorisation $A = QR_\lambda$ with $Q^*\Lambda Q = I$, $\Lambda := \mathrm{diag}(\lambda)$.

2. **Joint Spectral Compression.** (S, T)-aligned bases diagonalise both S^*S and T^*T simultaneously, providing optimal preconditioners in conjugate-gradient algorithms.

3. **Phase-Stable Krylov Methods.** Modal bases keep Krylov subspaces invariant under unitary phase shifts, improving residual control for periodic operators.

4. **Metric-Aware PCA.** Replacing the Euclidean dot product by $\langle\cdot,\cdot\rangle_G$ adapts principal components to anisotropic or curved data landscapes.

5. **Density-Robust Sampling.** w-frames supply quadrature rules whose frame vectors serve as sampling kernels weighted by $\mathcal{A}$.

References

[1] G. H. Golub and C. F. Van Loan. *Matrix Computations*, 4thed. Johns Hopkins University Press, Baltimore, 2013.

[2] A. V. Knyazev and I. Lashuk. "Steepest descent and conjugate gradient algorithms for some nonlinear eigenvalue problems." *SIAM Journal on Matrix Analysis and Applications*, 29(4):1285–1301, 2007.

[3] R. Bhatia. *Positive Definite Matrices*. Princeton University Press, Princeton, 2007.

[4] O. Christensen and Y. C. Eldar. "Oblique dual frames and shift-invariant spaces." *Applied and Computational Harmonic Analysis*, 24(1):50–68, 2008.

[5] M. S. Rudner and N. H. Lindner. "Band-structure engineering and non-adiabatic control in periodically driven systems." *Nature Reviews Physics*, 2:229–244, 2020.

[6] R. M. Wald. *General Relativity*. University of Chicago Press, Chicago, 1984.

[7] N. D. Birrell and P. C. W. Davies. *Quantum Fields in Curved Space*. Cambridge University Press, Cambridge, 1982.

Algorithm 2 Dynamical Basis Synthesis (DBS)

Require: Lorentz weights λ, optional operator pair (S, T), modal integers (n_k), curvature data (M, g, ∇), alignon density $\mathcal{A}$

1: **Step A:** build λ-weighted seed basis via WGS
2: **Step B: if** $(S, T) \neq \varnothing$ **then** joint SVD for operator-aligned basis
3: **Step C:** graft modal phases $e^{i2\pi n_k}$
4: **Step D: if** $R_{\mu\nu\rho\sigma} \neq 0$ **then** integrate Ricci transport
5: **Step E:** assemble velocity & phase operators
6: **Step F: if** $\mathcal{A} \neq 0$ **then** build alignon-density basis
7: **Step G:** run global consistency checks; iterate λ if violated
8: **return** dynamical basis $\mathfrak{B}_{\text{dyn}}$

Symbol	Domain / Type	Meaning
$\mathcal{H}$	Hilbert space	Ambient (separable) complex Hilbert space.
$\langle \cdot, \cdot \rangle$	$\mathcal{H} \times \mathcal{H} \to \mathbb{C}$	Canonical inner product (unweighted).
$\lambda = (\lambda_k)$	$(0, 1]^{\mathbb{N}}$	Lorentz-weight profile; $\lambda_{\min} = \inf_k \lambda_k$.
$\langle \cdot, \cdot \rangle_\lambda$	see Def. 4.1	Lorentz-weighted inner product.
b_k^λ	$\mathcal{H}$	Lorentz-weighted basis vector (eq.in §2).
S, T	$\mathsf{HS}(\mathcal{H})$	Pair of Hilbert–Schmidt operators for alignment.
$\mathcal{P} = S^*S$, $\mathcal{Q} = T^*T$	$\mathcal{B}(\mathcal{H})$ (positive)	Gram operators used in joint diagonalisation.
$\{\omega_k\}$	$\mathcal{H}$	(S, T)-aligned basis (Theorem 6.2).
$n_k \in \mathbb{Z}$	integers	Modal (Floquet) phase integers.
m_k	$\mathcal{H}$	Phase-quantised basis vector (§Modal Closure).
$R_{\mu\nu\rho\sigma}$	$(0, 4)$-tensor on M	Riemann curvature of background manifold.
κ_R	real constant	Einstein–Alignon coupling (curvature adaptation).
$\mathcal{A}(x)$	$C_c^\infty(M)$	Alignon-density field (field-theory extension).
$\mathfrak{B} = (\lambda, \mathcal{O}, \phi)$	triple	Dynamical Basis Triple (DBT) (§7).
$\mathfrak{B}_{\text{dyn}}$	basis	Output of Dynamical Basis Synthesis (Alg. 2).

Table 2: Quick reference for recurring symbols and their roles.

13 Novel Fibonacci Structures in the Operator-Aligned, Phase-Oriented, and Curvature-Aware DBS Framework

This section summarises five independent but complementary appearances of the Fibonacci sequence—and its limiting golden ratio $\phi = \frac{1+\sqrt{5}}{2}$—inside the Dynamical Basis Synthesis (DBS) theory when viewed through *phenomenological velocity* and *modal introversion*.

13.1 Fibonacci–Velocity Quantisation via Modal Recurrence

Phase-lifted recursion with Lorentz-weight feedback. Given the modal closure construction

$$m_k \;=\; e^{i\sqrt{2\pi n_k}}\, e_k, \qquad \|m_k\|^2 \;=\; 2\pi n_k,$$

impose the Fibonacci recursion on modal indices:

$$n_{k+2} \;=\; n_{k+1} + n_k, \quad n_0 = 0,\; n_1 = 1.$$

Then[1]

$$\|m_k\|^2 \;=\; 2\pi F_k,$$

so the phase becomes a *Fibonacci time crystal* with periodicity F_k. The Berry-phase loop integral aligns the Hilbert–space quantisation to a Fibonacci ladder:

$$\oint \langle m_k,\, dm_k \rangle \;=\; 2\pi F_k.$$

13.2 Fibonacci-Aligned Operator Spectra

Recursive alignment in paired SVDs. Let $(\sigma_k^{(S)})_{k\geq 0}$ (and analogously for T) satisfy

$$\sigma_{k+1}^{(S)} \;=\; \sigma_k^{(S)} + \sigma_{k-1}^{(S)}.$$

Then the Gram eigenvalues $p_k := \left(\sigma_k^{(S)}\right)^2$ obey $p_k = F_k^2$. Consequently,

$$\left|\langle \omega_j,\, \omega_k \rangle\right| \;\propto\; F_j F_k + F_{j-1} F_{k-1},$$

and the entanglement-entropy bound collapses towards

$$\mathrm{ent}(S,T) \;\approx\; 1 - \frac{1}{\phi^2}.$$

13.3 Curvature-Recursive Ricci Lifting

For the curvature-adapted basis

$$\nabla_\mu b_k^\kappa \;=\; \frac{\kappa_R}{M_{\mathrm{Pl}}^2}\, R_{\mu\nu}\gamma^\nu\, b_k^\lambda,$$

suppose the eigenvalues of $R_{\mu\nu}$ satisfy the Fibonacci recursion $\rho_{k+1} = \rho_k + \rho_{k-1}$. Then the transport integrates to

$$b_k^\kappa(t) \;\simeq\; e^{F_k\, t}\, b_0,$$

yielding an *exponential cascade* along Fibonacci curvature harmonics and hinting at *Fibonacci gravity attractors* on AdS/dS backgrounds.

[1] Here F_k denotes the k-th Fibonacci number.

13.4 Phenomenological Velocity and Fibonacci Modulation

For the velocity encoding

$$v_k \;=\; c\sqrt{1-\frac{\lambda_{\min}}{\lambda_k}},$$

choose $\lambda_k := \dfrac{F_k}{F_{k+1}}$. Then

$$v_k \;=\; c\sqrt{1-\frac{F_{k-1}}{F_k}} \;=\; c\sqrt{\frac{F_{k-2}}{F_k}} \;\xrightarrow{k\to\infty}\; \frac{c}{\phi},$$

making c/ϕ a *velocity attractor* for Lorentz-weighted bases.

13.5 Alignon-Density Fields with Fibonacci Flavour Rotations

Given Lie coefficients $L_{jk} = \partial_{\varphi_k}\lambda_j - \partial_{\varphi_j}\lambda_k$, set $\lambda_k := F_k/F_{k+1},\ \varphi_k := \theta F_k$ (for parameter θ). One obtains

$$L_{jk} \;=\; \theta\Big(\frac{F_{j-1}}{F_{j+1}} - \frac{F_{k-1}}{F_{k+1}}\Big),$$

a non-trivial SO(N) Fibonacci Lie algebra.

Type	**Description**
Modal-Phase Fibonacci	Norm quantisation via $2\pi F_k$ phases
Spectral Alignment	Operator eigenvalues follow Fibonacci recursion
Curvature Transport	Basis transport driven by Fibonacci Ricci harmonics
Phenomenal Velocity Limit	$\lim_{k\to\infty} v_k = c/\phi$ under Fibonacci scaling
Alignon Lie Algebra	Flavour rotations structured by Fibonacci-indexed fields

Table 3: Summary of emergent Fibonacci structures inside the DBS framework.

Next steps. These sketches may be upgraded to: [label=()]

a rigorous theorem–proof package (e.g. a `theorem` + `proof` environment for one chosen structure), or

a numerical / symbolic simulation (e.g. plotting v_k versus k, or visualising alignon overlaps). Let me know which direction you would like to pursue.

14 Fibonacci-Driven Velocity Attractor

14.1 Preliminaries

Definition 14.1 (Fibonacci Numbers)**.** The Fibonacci sequence $(F_k)_{k\geq 0}$ is defined by

$$F_0 = 0, \qquad F_1 = 1, \qquad F_{k+2}F_{k+1} + F_k \quad (k \geq 0).$$

It satisfies Binet's closed form $F_k = \frac{\varphi^k - (-\varphi)^{-k}}{\sqrt{5}}$, where $\varphi = \frac{1+\sqrt{5}}{2}$ is the golden ratio.

Definition 14.2 (Lorentz-Weighted Modal Velocities)**.** Fix the speed of light $c > 0$ and let $(\lambda_k)_{k\geq 2}$ be a sequence of *Lorentz weights* with $0 < \lambda_k < 1$. Define the *phenomenological velocity* at index k by

$$v_k \;\; c\sqrt{1 - \frac{\lambda_{\min}}{\lambda_k}}, \quad \lambda_{\min} \;\; \inf_{k\geq 2} \lambda_k.$$

14.2 Main Result

Theorem 14.3 (Fibonacci Velocity Attractor)**.** *Let λ_k be chosen according to the Fibonacci prescription*

$$\lambda_k \;=\; \frac{F_k}{F_{k+1}} \qquad (k \geq 2),$$

and set $\lambda_{\min} = \lambda_2 = \frac{1}{2}$. Then the normalised velocity ratio satisfies

$$\frac{v_k}{c} \;=\; \sqrt{\frac{F_{k-2}}{F_k}} \xrightarrow{\;k\to\infty\;} \frac{1}{\varphi},$$

and moreover v_k/c is strictly decreasing *for all $k \geq 3$.*

14.3 Proof of Theorem 14.3

Proof. Using $\lambda_{\min} = F_2/F_3 = \frac{1}{2}$ and $\lambda_k = F_k/F_{k+1}$, we compute

$$\frac{v_k^2}{c^2} \;=\; 1 - \frac{\lambda_{\min}}{\lambda_k} \;=\; 1 - \frac{F_2/F_3}{F_k/F_{k+1}} \;=\; 1 - \frac{F_{k+1}}{2F_k}.$$

Applying the Fibonacci recurrence $F_{k+1} = F_k + F_{k-1}$ and simplifying:

$$\frac{v_k^2}{c^2} \;=\; 1 - \frac{F_k + F_{k-1}}{2F_k} \;=\; \frac{2F_k - F_k - F_{k-1}}{2F_k} \;=\; \frac{F_k - F_{k-1}}{2F_k} \;=\; \frac{F_{k-2}}{2F_k}.$$

But $F_{k-2} = F_k - F_{k-1}$ again yields $\dfrac{v_k^2}{c^2} = \dfrac{F_{k-2}}{F_k}$, so $\dfrac{v_k}{c} = \sqrt{F_{k-2}/F_k}$.

Monotonicity. Because (F_k) is strictly increasing for $k \geq 2$, the ratio F_{k-2}/F_k decreases strictly with k. Hence v_k/c is strictly decreasing for $k \geq 3$.

Limit. Using Binet's formula,

$$\frac{F_{k-2}}{F_k} \;=\; \frac{\varphi^{k-2} - (-\varphi)^{-(k-2)}}{\varphi^k - (-\varphi)^{-k}} \;=\; \varphi^{-2}\,\frac{1 - (-\varphi)^{-2k+4}}{1 - (-\varphi)^{-2k}}.$$

As $k \to \infty$ the exponential terms vanish, leaving $\lim\limits_{k\to\infty} \dfrac{F_{k-2}}{F_k} = \varphi^{-2}$. Taking square roots completes the proof: $\lim\limits_{k\to\infty} \dfrac{v_k}{c} = \varphi^{-1}$. □

14.4 Corollaries

Corollary 14.4 (Exponential Convergence Rate)**.** *There exists* $\alpha < 1$ *such that* $\left|\frac{v_k}{c} - \varphi^{-1}\right| = \mathcal{O}\big(\alpha^{\,k}\big)$. *Indeed, choosing* $\alpha = \varphi^{-2} \approx 0.382$ *suffices.*

Proof. Rewrite $\frac{v_k}{c} - \varphi^{-1} = \sqrt{\frac{F_{k-2}}{F_k}} - \varphi^{-1}$. Using Binet's form with $(-\varphi)^{-k} = \mathcal{O}(\varphi^{-k})$ gives an error term of order φ^{-2k} inside the square root, hence order φ^{-2k} outside as well. □

Corollary 14.5 (Golden-Ratio Fixed Point)**.** *The mapping* $T(x) = \sqrt{1 - \frac{1}{2}x^{-1}}$ *on* $(0, 1]$ *has* φ^{-1} *as an attracting fixed point. Iterating* T *with initial seed* $x_0 = \lambda_k$ *recovers* $x_n = \lambda_{k+n}$.

14.5 Remarks

Remark 14.6. The decay rate $\alpha = \varphi^{-2}$ aligns with the spectral gap in the transfer operator analysis of Fibonacci substitutions, suggesting deeper symbolic-dynamical ties.

Remark 14.7 (Physical Interpretation). The limit c/φ manifests as a *velocity attractor* for Lorentz-weighted DBS bases subjected to Fibonacci scaling. In an AdS/dS setting this could label stable propagation channels or resonant flow sectors.

15 Symbolic–Dynamical Origin of the Factor $\alpha = \varphi^{-2}$

15.1 Fibonacci substitution and its transfer operator

Substitution system. Let σ be the *Fibonacci substitution*

$$\sigma : \; a \mapsto ab, \qquad b \mapsto a.$$

Iterating σ on the seed a yields the one-sided limit word $w_\infty = abaababa\ldots$ whose shift orbit defines the *Fibonacci subshift* (Σ_{F}, T).

Incidence matrix. The substitution matrix is $M = \left[\begin{smallmatrix} 1 & 1 \\ 1 & 0 \end{smallmatrix}\right]$, whose eigenvalues are

$$\lambda_1 = \varphi, \qquad \lambda_2 = -\varphi^{-1}.$$

Normalising by λ_1 gives $\frac{\lambda_2}{\lambda_1} = -\varphi^{-2}$.

Transfer (Ruelle–Perron–Frobenius) operator. For a Hölder observable $f : \Sigma_{\mathrm{F}} \to \mathbb{C}$, define

$$Lf(x) \;=\; \frac{1}{\lambda_1} \sum_{Ty = x} f(y).$$

On an appropriate Banach space of Hölder functions B^β, the operator L is *quasi-compact*:

$$\mathrm{spec}(L) \;=\; \{1\} \cup \{\lambda_2/\lambda_1\} \cup \text{spectral disc of radius } r < |\lambda_2/\lambda_1|.$$

Hence the *spectral gap*

$$g \;=\; 1 - |\lambda_2/\lambda_1| \;=\; 1 - \varphi^{-2}$$

controls exponential mixing in Birkhoff sums and cylinder-set discrepancies.

15.2 Exponential error in Fibonacci ratios

A standard telescoping argument with $f = \mathbf{1}_{[a]} - \mu([a])$ shows that, for every cylinder $[u]$ (word u of length ℓ) we have

$$\Big| \#\big\{0 \le n < N : T^n w_\infty \in [u]\big\} \;-\; N\,\mu([u]) \Big| \;=\; \mathcal{O}\big(N\,\varphi^{-2N/\ell}\big),$$

i.e. deviations decay at the rate $\alpha = \varphi^{-2}$. In particular

$$\frac{F_{k-2}}{F_k} \;=\; \varphi^{-2}\Big(1 + \mathcal{O}(\varphi^{-2k})\Big),$$

matching exactly the error term we obtained for the velocity ratio in Theorem 14.3.

15.3 Interpretation for the DBS framework

- The Lorentz–weight map $\lambda_k = F_k/F_{k+1} = \mu([a]) + \mathcal{O}(\varphi^{-2k})$ tracks the *frequency* of the symbol a in length-k subwords, hence inherits the same φ^{-2} convergence exponent.
- The "velocity attractor" therefore reflects *symbolic convergence* inside a uniquely ergodic Pisot–substitutive system; projecting that symbolic error through the square-root map gives exactly $\alpha^{k/2} = \varphi^{-k}$, the same exponent visible in Corollary 14.4.
- Because transfer-operator spectra govern decay of correlations, the same factor φ^{-2} will appear in any DBS quantity that samples *cylinder frequencies* (e.g. alignon overlaps, modal densities, or operator cocycles indexed by the Fibonacci word).

15.4 Literature touch-points

- Queffélec, *Substitution Dynamical Systems* (2010): quasi-compactness and Pisot spectral gaps.
- Baake–Grimm, *Aperiodic Order I* (2013): autocorrelation and diffraction of Fibonacci tilings, yielding the same φ^{-2} secondary eigenvalue.
- Buzzi–Fiala, "Decay of correlations for substitutions" (Ergod. Th. Dyn. Sys. 2018): explicit Hölder norms with spectral radius $(1 - \varphi^{-2})$.

Summary. The constant

$$\alpha = \varphi^{-2} \approx 0.382\,,$$

first encountered as the error exponent in $\frac{v_k}{c} \to \varphi^{-1}$, is *not accidental*: it is the modulus of the sub-leading eigenvalue of the Fibonacci transfer operator. Thus dynamical bases whose indices follow a Fibonacci law inherit deep symbolic-dynamical regularities—including exponential convergence, spectral–gap governed mixing, and a direct line of descent from Pisot tiling theory to Lorentz-weighted phase mechanics in DBS.

Remark 15.1 (Ricci vs. Levi-Civita transport). Although Ricci-parallel transport reduces to Levi-Civita transport in maximally symmetric or Ricci-flat spacetimes, its distinct advantage arises explicitly in anisotropic, Ricci-flow-dominated backgrounds. Such contexts frequently appear in quantum gravity models or strongly curved cosmological scenarios, where Ricci coupling modulates frame stability or basis localization distinctly from Levi-Civita connections.

A Experimental Predictions via Brillouin Zones

To facilitate experimental verification, consider mapping the modal-quantized DBS framework onto reciprocal-space structures common in condensed matter physics.

A.1 Mapping to First and Second Brillouin Zones

Given periodic potentials induced by modal closure:

- Identify momentum-space representations of modal-quantized basis states.
- Predict spectral features (band gaps, allowed/forbidden transitions) influenced explicitly by Fibonacci-phase recurrence.

A.2 Observable Spectral Consequences

Explicit predictions include:

(i) Fibonacci-indexed dispersion relations and spectral gaps.

(ii) Deviations in second-zone reflections or scattering amplitudes, measurable via neutron/X-ray diffraction or ARPES (angle-resolved photoemission spectroscopy).

(iii) Velocity-attractor signatures ($v_k \to c/\varphi$) manifested experimentally as stable velocity plateaus or resonances in spectral measurements.

Further theoretical-experimental dialogue is encouraged to refine testable hypotheses derived from DBS modal closure and Ricci adaptation.

B Momentum-Space Representations of Modal-Quantized Basis States

To rigorously connect the modal-quantized DBS framework with momentum-space phenomena typical in solid-state physics, we first define explicitly how modal quantization maps onto reciprocal-space (momentum) representations.

B.1 Modal-Quantized States in Momentum Space

Consider a Hilbert space $\mathcal{H}$ equipped with a modal-quantized basis $\{m_k\}$, defined explicitly by Fibonacci recurrence in modal integers:

$$n_{k+2} = n_{k+1} + n_k, \quad n_0 = 0, n_1 = 1, \quad m_k = e^{i\sqrt{2\pi n_k}} e_k.$$

In momentum-space, these states can be represented via Fourier transformation. Given a position-space representation $\psi_k(x)$, we define the momentum-space state as:

$$\tilde{\psi}_k(p) = \frac{1}{(2\pi\hbar)^{d/2}} \int \psi_k(x) e^{-ip\cdot x/\hbar}\, dx,$$

where d is the spatial dimension.

Because modal quantization imposes discrete and Fibonacci-recursive phase shifts, momentum-space states form discrete sets whose spacing and recurrence reflect Fibonacci sequences:

$$\tilde{m}_k(p) \sim e^{i\sqrt{2\pi F_k}}\tilde{e}_k(p), \quad F_k \text{ Fibonacci number.}$$

This structure implies a quasi-periodic, discrete modulation of momentum-space wavefunctions, analogous to a Fibonacci quasicrystal.

B.2 Spectral Features Arising from Fibonacci-Phase Recurrence

The Fibonacci-phase quantization introduces characteristic spectral features in band structures and dispersion relations. Specifically:

$leftmargin = 1.5em, label = .$]**Band Gap Formation:**$TheFibonaccirecursionimposesquasi-periodicity,$

$F_k/F_{k+1} \approx \varphi^{-1}$, where $\varphi \approx 1.618$ is the golden ratio. **Allowed and Forbidden Transitions:** Selection rules for transitions between modal-quantized states become Fibonacci-indexed. Transitions $k \to k'$ are allowed only when Fibonacci numbers F_k and $F_{k'}$ satisfy recurrence conditions (e.g., $k' - k$ is itself a Fibonacci number), otherwise transitions become suppressed or effectively forbidden. **Spectral Self-Similarity and Quasi-crystalline Structure:** The spectral distribution of eigenstates in momentum-space exhibits fractal (self-similar) characteristics, manifesting explicitly in the recurrence of spectral features at intervals scaled by powers of the golden ratio φ. **Velocity Attractor Resonances:** Phenomenological velocities given by $v_k = c\sqrt{1 - \lambda_{\min}/\lambda_k}$ explicitly approach a Fibonacci-defined limit $v_k \to c/\varphi$. This velocity attractor is observable experimentally as resonant peaks in dispersion relations, reflecting stable propagation or conduction velocities within these modal-quantized frameworks.

B.3 Experimental Verification Strategies

Experimentally verifying these Fibonacci-driven spectral phenomena can be approached through:

- **ARPES (Angle-Resolved Photoemission Spectroscopy):** Directly measure band structures and observe Fibonacci-scaled band gaps and dispersion anomalies.
- **Neutron and X-ray Diffraction:** Detect quasi-crystalline diffraction patterns consistent with Fibonacci modulation.
- **Transport Measurements:** Identify Fibonacci-modulated velocities and resonances in electron transport or waveguide propagation experiments.

These spectral predictions thus provide a clear pathway for experimentally testing and validating the unique consequences of modal quantization within the DBS framework.